Engineered off-the-shelf therapeutic T cells resist host immune rejection

Feiyan Mo[1,2], **Norihiro Watanabe**[1], **Mary K McKenna**[1], **M. John Hicks**[3], **Madhuwanti Srinivasan**[1], **Diogo Gomes-Silva**[1], **Erden Atilla**[1], **Tyler Smith**[1], **Pinar Ataca Atilla**[1], **Royce Ma**[1,4], **David Quach**[1], **Helen E. Heslop**[1,2], **Malcolm K. Brenner**[1,2], **Maksim Mamonkin**[1,2,3,4,*]

[1]Center for Cell and Gene Therapy, Baylor College of Medicine, Texas Children's Hospital and Houston Methodist Hospital, Houston, TX

[2]Graduate Program in Translational Biology and Molecular Medicine, Baylor College of Medicine, Houston, TX

[3]Department of Pathology and Immunology, Baylor College of Medicine, Houston, TX

[4]Graduate Program in Immunology, Baylor College of Medicine, Houston, TX

Engineered T cells are effective therapies against a range of malignancies, but current approaches rely on autologous T cells, which are difficult and expensive to manufacture. Efforts to develop potent allogeneic T cells that are not rejected by the recipient's immune system require abrogating both T- and NK-cell responses, which eliminate foreign cells through various mechanisms. Here, we engineered a receptor that mediates deletion of activated host T and NK cells, preventing rejection of allogeneic T cells. Our alloimmune defense receptor (ADR) selectively recognizes 4-1BB, a cell surface receptor temporarily upregulated by activated lymphocytes. ADR-expressing T cells resist cellular rejection by targeting alloreactive lymphocytes *in vitro* and *in vivo,* while sparing resting lymphocytes. Cells co-expressing chimeric antigen receptors (CAR) and ADR persisted in mice and produced sustained tumor eradication in two mouse models of allogeneic T-cell therapy of hematopoietic and solid cancer. This approach enables generation of rejection-resistant "off-the-shelf" allogeneic T-cell products to produce long-term therapeutic benefit in immunocompetent recipients.

Main

Autologous therapeutic T cells, such as chimeric antigen receptor (CAR) T cells and T cell receptor (TCR) engineered T cells, have successfully treated malignancies and infectious diseases in many patients[1-3] but require complex patient-specific manufacturing, which limits scalability and can result in therapeutic products with unpredictable potency[4]. Well characterized, banked therapeutic cells pre-manufactured from healthy donors could address these limitations, offering immediate availability and high potency at a reduced cost. To achieve full therapeutic benefit, unwanted graft-versus-host and host-versus-graft activities promoted by infusion of allogeneic T cells must be mitigated[4]. Potential graft-versus-host reactivity of allogeneic T cells can be minimized by disrupting TCR expression[5-9] or by selecting T cells with defined specificity to non-self (i.e., viral) antigens[10-12]. However, alloimmune rejection by host lymphocytes and the development of alloimmune memory may limit the persistence of infused cells and minimize the benefit of additional cell doses.

Initial stimulation of resting T and NK cells via the TCR and other receptors produces a transient activation state characterized by acquisition of cytotoxic mechanisms and other effector functions. Activated lymphocytes temporarily upregulate several surface receptors, such as 4-1BB (CD137), that can provide additional costimulation[13]. After activation subsides, many of these molecules are rapidly downregulated and thus can serve as markers distinguishing activated cytotoxic effector cells from unstimulated populations. We hypothesized that selective elimination of 4-1BB-expressing activated T and NK cells by allogeneic therapeutic T cells may suppress cellular rejection and extend their functional activity without ablating non-alloreactive host lymphocytes.

Here, we engineered a chimeric 4-1BB-specific alloimmune defense receptor (ADR) that enables therapeutic T cells to selectively target activated T and NK cells. We show that ADR-expressing T cells spare resting T and NK cells and evade immune rejection by eliminating alloreactive lymphocytes, and co-expression of ADR with CARs in T cells promote durable anti-tumor activity in mouse models of allogeneic T-cell therapy of cancer.

Results

4-1BB-specific ADR enables T cells to selectively recognize activated T and NK cells

Cellular immune rejection is mediated by activated alloreactive T and NK cells of the host[14-17]. We hypothesized that selective depletion of cytotoxic lymphocytes in the transient state of activation will suppress immune rejection of infused therapeutic cells. 4-1BB is upregulated on the cell surface of activated CD4$^+$ and CD8$^+$ T cells, as well as NK cells (Supplementary Fig. 1a, b), marking these subsets for selective recognition. Immunohistochemistry analysis showed no 4-1BB expression in normal human tissues apart from tonsils, a site of continuous immune activation (Supplementary Fig. 2a, b). We engineered a 4-1BB-specific chimeric alloimmune defense receptor (ADR) consisting of a 4-1BBL-derived recognizing fragment connected via spacer and transmembrane regions to the intracellular CD3ζ chain covalently fused with a fluorescent tag mEmerald (Fig. 1a). Following gammaretroviral transduction, ADR was expressed on the cell surface of primary human T cells and did not abrogate subsequent T-cell expansion (Fig. 1b, c). ADR-

expressing T cells specifically eliminated 4-1BB-expressing cells but not 4-1BB-negative controls (Fig. 1d, Supplementary Fig. 1c, d). We observed no reactivity of ADR T cells against freshly isolated resting CD4$^+$ and CD8$^+$ T cells and NK cells (Fig. 1e, f). In contrast, ADR T cells were cytotoxic against pre-activated T- and NK cells (Fig. 1e, f) and demonstrated higher potency against activated CD8$^+$ T cells, likely due to their increased expression of 4-1BB (Supplementary Fig. 1a). ADR T cells produced minimal degranulation in the absence of target cells but degranulated upon coculture with activated allogeneic T cells (Supplementary Fig. 3a-c). Target cell killing by ADR T cells was mediated by both the Fas-dependent and granzyme B/perforin-dependent pathways (Supplementary Fig. 3d).

ADR-armed T cells are protected from T- and NK-cell mediated rejection in vitro

We used mixed lymphocyte reaction (MLR) models to evaluate the ability of ADR T cells to eliminate alloreactive cytotoxic lymphocytes and resist immune rejection *in vitro*. To model an "off-the-shelf" T-cell product with minimal graft-versus-host reactivity, we disrupted surface expression of TCR using genome editing (TCR^{KO} T cells). HLA-A2$^+$ T cells were TCR-edited by electroporation with Cas9 complexed with a CD3ε-specific sgRNA. TCR expression was disrupted in >90% of cells that were further enriched to >99% purity using magnetic beads (Supplementary Fig. 4). TCR^{KO} T cells from HLA-A2$^+$ donors were co-cultured with a 10-fold excess of peripheral blood mononuclear cells (PBMC) from HLA-mismatched recipients (Fig. 2a). In this model, recipient T and NK cells expanded and eliminated donor T cells within 9-12 days (Fig. 2b-d). Expression of ADR protected donor T cells from elimination and promoted their expansion in response to ADR stimulation. ADR T cells controlled the expansion of recipient lymphocytes, enabling the coexistence of both donor and recipient effector populations (Fig. 2c, d).

To further dissect the activity of ADR against alloreactive cytotoxic lymphocytes, we cocultured control non-transduced and ADR-expressing T cells with NK-depleted PBMC where alloimmune rejection was mediated primarily by recipient T cells (Fig. 2e). While unmodified T cells were rejected after 9-12 days of coculture, ADR-modified T cells were protected from elimination and controlled the expansion of recipient T cells for the duration of the experiment (Fig. 2f-h). Further, ADR expression protected donor T cells from rejection by purified alloreactive recipient T cells previously primed with irradiated donor T cells (Fig. 2i-l) indicating ADR T cells act directly against targeted T cells.

To model NK-cell mediated rejection, we ablated the expression of beta-2 microglobulin (β2m) on donor T cells, which results in a loss of surface MHC class I molecules, suppressing recognition by T cells but promoting activation of NK cells[7,18,19]. Indeed, β2m-edited control T cells were completely eliminated by allogeneic PBMC within 6 days, resulting in an expansion of recipient NK cells (Fig. 3a-d). In contrast, β2m-edited ADR T cells resisted immune rejection and suppressed NK-cell expansion. Further, we co-cultured β2m-edited T cells with purified allogeneic NK cells at a 1:1 cell ratio, which resulted in rejection of T cells within 2-3 days. Expression of ADR on β2m-edited T cells prevented this rejection, maintaining the initial effector-to-target ratio (Fig. 3e-h). Therefore, the expression of ADR enables T cells to resist alloimmune rejection mediated by T- and NK cells.

ADR protects T cells from alloimmune cellular rejection in vivo

Next, we established *in vivo* models of alloimmune rejection by engrafting sublethally irradiated NSG mice with HLA-A2$^+$ (recipient) T cells intravenously followed by intravenous administration of HLA-A2$^-$ (donor) T cells 4 days later (Fig. 4a and Supplementary Fig. 5-6). In this model, donor T cells were eliminated in all animals by day 18. To confirm immune rejection of donor T cells, we re-challenged animals with a 1:1 mix of CFSE-labeled recipient (HLA-A2$^+$) and donor (HLA-A2$^-$) T cells and analyzed the ratio of CFSE$^+$ donor and recipient cells in peripheral blood and spleen 48h later. Donor T cells were selectively depleted in mice that previously received T cells from the same donor, but not in control mice that had not received donor T cells prior (Supplementary Fig. 5). These results demonstrate the development of alloreactive memory specific to HLA-A2$^-$ cells. Notably, arming donor T cells with ADR enabled them to withstand allogeneic rejection and expand in the presence of allogeneic T cells (Fig. 4b, c), mirroring the behavior observed in MLR models. Again, ADR T cells did not eliminate all recipient T cells but instead co-engrafted in mice and established long-term persistence alongside the allogeneic population (Fig. 4d). To evaluate whether the persisting recipient T cells retain alloreactivity against donor cells, HLA-A2$^+$ recipient T cells were purified from spleens of mice on day 81 after ADR T-cell injection and co-cultured for 72h with a 1:1 mix of TCR^{KO} T cells from the same donor-recipient pair (Fig. 4e and Supplementary Fig. 6a). Whereas control recipient T cells previously primed by HLA-A2$^-$ donor cells selectively ablated donor T cells, we observed no selective reactivity by recipient T cells isolated from four individual mice against HLA-A2$^-$ T cells at the end of co-culture indicating absence of donor-specific alloreactivity in persisting recipient T cells (Fig. 4e). Recipient T cells retained TCR-driven cytotoxic function as reflected by elimination of K562 cells expressing an anti-CD3 single-chain variable fragment (K562.OKT3) (Supplementary Fig. 6b).

In order to assess both T- and NK-cell responses, we substituted allogeneic recipient T cells with whole PBMC in this mouse model. To reduce graft-versus-host reactivity of human cells, we engrafted recipient human PBMC into mice lacking MHC class I and class II genes[20] followed by intravenous administration of donor T cells (Fig. 4f). Similar to the previous model, unmodified donor T cells were rejected by expanding recipient PBMC within 2 weeks whereas ADR T cells proliferated, persisted, and suppressed the expansion of recipient PBMC (Fig. 4g-i). Collectively, these results indicate ADR-expressing T cells suppress cellular alloimmune rejection.

T cells co-expressing ADR and CD19 CAR retain specific activity via both receptors

Expression of ADR on allogeneic CAR T cells could suppress host immune rejection and extend their anti-tumor activity. In order to test whether ADR- and CAR-expressing T cells retain independent anti-rejection and anti-tumor functions, we co-expressed ADR with a second-generation CD19 CAR on T cells (Fig. 5a) by co-transducing them with separate gammaretroviral vectors encoding CAR and ADR. We evaluated the ability of these CAR.ADR T cells to eliminate tumor cells (via CAR) and activated T cells (via ADR) *in vitro*. T cells expressing both CD19 CAR and ADR were highly cytotoxic against CD19$^+$ NALM6 cells, similar to positive controls expressing CD19 CAR alone (Fig. 5b). Likewise, co-culture with activated T cells resulted in a comparable decrease in target cell counts by

ADR-only and CAR.ADR T cells (Fig. 5c). Next, we assessed the ability of CAR.ADR T cells to exert function through both receptors simultaneously. Co-culture of CAR.ADR T cells with NALM6 and activated T cells in the same dish resulted in a significant reduction of both types of targets, to the same extent as the single-receptor control T cells (Fig. 5d). These results indicate ADR and CAR preserve their independent anti-rejection and anti-tumor activities when co-expressed in T cells.

CD19 CAR.ADR T cells overcome immune rejection and eliminate leukemia in vivo

We evaluated the function of CAR.ADR T cells in a mouse model of disseminated B-cell leukemia in which CAR T cells must resist immune rejection from allogeneic T cells while protecting mice against cancer progression. We adapted our previous mouse model to engraft CD19$^+$ NALM6 B-ALL cells, one day after the administration of recipient T cells (RTC, Fig. 6a). To avoid nonspecific allogeneic rejection by T cells, we deleted MHC class I expression from tumor cells. Three days later, mice received a single dose of 2×10^6 donor CD19 CAR and/or ADR-expressing T cells intravenously (Fig. 6a).

In the absence of recipient T cells, CD19 CAR T cells eliminated pre-established tumors and persisted long-term in many animals (Fig. 6b, d, e; green lines). However, in the presence of recipient T cells, CD19 CAR T cells were rapidly rejected in 19 out of 20 mice (Fig. 6b; red lines) resulting in expansion of recipient (HLA-A2$^+$) T cells in peripheral blood (Fig. 6c). The kinetics of recipient T-cell expansion was delayed in mice receiving less cytoablation (0.8Gy; open circles), likely due to reduced initial engraftment and increased competition with donor CAR T cells (Fig. 6c). Early loss of CD19 CAR-T cells resulted in only transient anti-tumor activity, ultimately leading to fatal relapses in all mice (Fig. 6d, e). T cells expressing ADR alone were able to suppress the expansion of recipient T cells and resist immune rejection but failed to protect the mice against systemic leukemia (Supplementary Fig. 7). In contrast, co-expression of ADR on CD19 CAR T cells resulted in their systemic expansion and persistence (Fig. 6b; purple lines) alongside recipient T cells (Fig. 6c). This expansion was not autonomous as CAR- and ADR-expressing T cells failed to expand in mice in the absence of their respective target antigens (Supplementary Fig. 8). Notably, long-term expansion of CAR.ADR T cells exceeded that of CD19 CAR T cells in the absence of RTC. This difference was especially evident in animals receiving a higher dose of pre-treatment cytoablation (1.2Gy; solid circles) that promoted more robust expansion of recipient T cells, suggesting dual stimulation through both CAR and ADR is beneficial for *in vivo* proliferation and survival. As a result, sustained eradication of leukemia was observed in 17 out of 19 animals (Fig. 6d), translating to long-term survival in most CAR.ADR-treated mice (Fig. 6e).

Expansion of activated CAR.ADR T cells *in vivo* indicates these cells evade 4-1BB directed self-targeting. We found activated CD19 CAR.ADR T cells have lower levels of detectable 4-1BB on their surface compared to CD19 CAR T cells, suggesting partial downregulation or masking of 4-1BB upon ADR expression (Supplementary Fig. 9a). Indeed, expression of a truncated non-signaling ADR on activated T cells protected them from cytotoxicity by ADR T cells (Supplementary Fig. 9b-d) so that *cis*-masking of 4-1BB by ADR likely contributes to fratricide resistance of activated ADR T cells.

GD2 CAR.ADR T cells eradicated systemic neuroblastoma and resisted alloimmune rejection

We used a mouse xenograft model of metastatic $GD2^+$ neuroblastoma[21] where mice received CHLA-255 cells and T cells expressing GD2 CAR and/or ADR. Unarmed GD2 CAR T cells were rejected by pre-engrafted recipient T cells, and mice developed early relapses but also severe xenogeneic GvHD that required early euthanasia of all animals (Supplementary Fig. 10). In contrast, a single administration of donor GD2 CAR.ADR T cells resulted in long-term T-cell expansion and sustained eradication of neuroblastoma (Supplementary Fig. 10).

Prevention of both graft-versus-host and host-versus-graft activities by combining ADR with TCR deletion

To model an off-the-shelf T-cell product, we expressed CD19 CAR on TCR-edited T cells and evaluated whether ADR expression would protect these cells from allogeneic rejection. Co-transduction of TCR^{KO} T cells with gammaretroviral vectors encoding CD19 CAR and ADR resulted in >75% of cells co-expressing both chimeric receptors (Supplementary Fig. 11). TCR-edited CD19 CAR T cells alone controlled NALM6 leukemia, although in most mice the cells became undetectable after 30 days, coinciding with late leukemia relapses in some animals (Fig. 6f, g, i; green lines). As expected, the presence of allogeneic recipient T cells curtailed the persistence and activity of unarmed TCR^{KO} CD19 CAR T cells, resulting in rapid relapses and shortened survival in 22 out of 23 mice (Fig. 6g-j; red lines). Arming TCR^{KO} CD19 CAR T cells with ADR significantly increased their expansion and persistence in peripheral blood, while limiting the expansion of recipient T cells, eradicating leukemia in 20 out of 21 animals (Fig. 6g-j; purple lines), and prolonging tumor-free survival.

Discussion

We show that T cells armed with a 4-1BB specific alloimmune defense receptor selectively target activated alloreactive T and NK cells and suppress immune rejection *in vitro* and *in vivo*. Similarly, CAR T cells co-expressing ADR resist immune rejection and retain potent anti-tumor activity in mouse xenograft models of human hematological and solid malignancies. These results support the development of off-the-shelf ADR.CAR T-cell products resistant to host immune rejection.

Several strategies have been developed to limit immune recognition of engineered cell products. Surface expression of chimeric receptors, particularly with non-human derived (e.g., murine) sequences, was shown to elicit B-cell mediated responses in some patients that promoted the generation of human anti-mouse antibodies[22,23]. These B-cell responses can be suppressed in patients receiving CAR-T cells targeting B-cell antigens, such as CD19. Further "humanization" of chimeric receptors by grafting murine antigen-binding sequences onto human framework regions or by using fully human-derived targeting moieties can reduce xenogeneic B- and T-cell responses[24]. However, preventing cellular rejection of allogeneic, MHC-mismatched cells by host T and NK cells requires additional engineering strategies.

Disrupting the expression of MHC Class I alleles by knocking out the β2m gene, which is required to stabilize the expression of all MHC class I molecules on the cell surface, is one such strategy that has been widely evaluated in preclinical models[7,18]. This approach alone, or in combination with targeting MHC Class II alleles, reduces T-cell recognition of allogeneic cells but potentiates activation of NK cells through the multitude of activating receptors not counteracted by inhibitory signals from MHC-sensing inhibitory molecules[19].

Due to the heterogeneity of NK-cell subsets expressing a broad repertoire of activating and inhibitory receptors, designing a molecular system with a broad, pan-NK cell inhibitory function can be difficult. For example, forced expression of HLA-E[18,25], a non-classical MHC class I molecule, was shown to inhibit NK cells by binding to NKG2A/B receptors[26-28]. However, this approach would be effective only against a subset of NK cells expressing the respective receptors and may also stimulate some NK cells via activating receptor NKG2C[26]. Non-specific elimination of host lymphocytes by alemtuzumab can suppress cellular rejection of the infused product but leads to severe immunosuppression and requires additional genetic disruption of the gene encoding CD52, a target antigen of alemtuzumab, to protect the adoptively transferred T cells[9].

In contrast, ADR redirects cytotoxic therapeutic T cells to eliminate alloreactive T- and NK cells in their transient activation state. Moreover, ADR T cells retain normal expression of MHC, which may reduce NK-cell activation compared to MHC-deleted T cells. Because activated B-cells[29,30], follicular DCs[31] and follicular helper T cells[32] also express 4-1BB transiently, future studies may evaluate whether 4-1BB ADR-armed T cells suppress unwanted alloimmune B-cell responses specific to donor HLA or other allogeneic target molecules.

While 4-1BB expression was not detected in non-lymphoid tissues, the molecule is reported to be transiently upregulated upon activation on subsets of monocytes[29], eosinophils[33], and mast cells[34], potentially exposing them to ADR T cells. These non-critical myeloid cells are continuously replenished and therefore their transient depletion should be tolerable and would contribute to suppressing alloimmune priming and dampen anti-donor cytotoxic response. It is also possible that ADR activity may result in a temporary suppression of productive systemic T-cell responses (e.g., tumor- or pathogen-specific). While we cannot rule out this unwanted activity, the extent of suppression will likely be limited by the following factors. First, some pathogen-specific memory cell subsets, such as effector memory[35] and tissue-resident memory[36,37] T cells, do not require transitioning to an activated state prior to exerting effector functions. Coculture of multivirus-specific T cells (VST) with ADR T cells decreased VST counts in an ADR-T:VST cell ratio-dependent manner but did not abrogate VST cytotoxicity against autologous lymphoblastoid cell lines pulsed with viral peptides (Supplementary Fig. 12). Second, not all activated T cells may stably upregulate 4-1BB, as evidenced by the presence of activated T cells resistant to ADR cytotoxicity in our *in vitro* and *in vivo* assays, as well as by the fact that ADR T cells have very limited fratricide and eventually become resistant to self-directed killing. Third, while cellular rejection requires co-localization of allogeneic cells and activated alloreactive lymphocytes, pathogen-specific host T-cell responses may be spatially separated from ADR T cells and would thus be spared. Indeed, clinical studies of CAR T cells specific to CD30

— another marker upregulated on activated T cells — show no evidence of systemic immunosuppression or increased frequency of infections[38]. Limitations of mouse models used in this study did not allow fully investigating the effect of ADR T cells on concurrent immune responses. Ultimately, safety and efficacy of ADR-expressing allogeneic effector cells will be assessed in dose-escalation clinical studies with access to all mitigating strategies to manage potential dose-limiting toxicities commonly occurring with other CAR T-cell products.

We expected that expression of 4-1BB on activated ADR T cells would cause fratricide and, indeed, we saw a transient reduction in numbers of ADR T cells upon coculture with target cells *in vitro* and in our *in vivo* models. However, this self-directed cytotoxicity was always transient, with a fratricide-resistant population of functional ADR T cells expanding and persisting. Activation-induced upregulation of 4-1BB on ADR T cells can be partially masked from surrounding cells by binding ADR in *cis* on the cell surface. A similar mechanism was recently demonstrated in CD19⁺ B-cell leukemia expressing a CD19 CAR[39]. Such *cis* engagement of 4-1BB in ADR T cells may promote additional costimulatory signaling in T cells to increase their proliferation and survival, as was shown in other preclinical models[40-42]. These processes likely contribute to emergence of a fratricide-resistant population of ADR T cells.

Targeted elimination of pathogenic lymphocytes can be beneficial in certain autoimmune conditions, solid organ rejection, and GvHD. The effect of targeting 4-1BB and other T-cell activation markers using ADR T cells in those indications can be evaluated separately.

In conclusion, we developed a first-in-class alloimmune defense receptor targeting 4-1BB for selective elimination of the pathogenic T and NK cells that mediate cellular rejection of allogeneic therapeutic T cells. This chimeric receptor may prolong the persistence and antitumor function of off-the-shelf T cells in non-immunocompromised patients without ablating the lymphocyte compartment. Overall, our approach provides a simple yet effective alternative to other methods of cell engineering directed at reducing recognition of therapeutic cells by host cellular immunity.

Methods

Constructs

Ligand-binding fragment of human 4-1BBL was PCR-amplified from human cDNA library and fused with a backbone containing a custom spacer, transmembrane region and CD3z domain covalently linked with mEmerald[43] using InFusion cloning (Takara Bio) and verified using Sanger sequencing. Amino acid sequence of the 4-1BBL-based ADR binder is indicated in Supplementary Fig. 13. The ΔADR construct was cloned by removing intracellular domains of the full-length ADR using InFusion cloning. A second-generation CD19.BBz CAR, consisting of a CD19-specific scFv (FMC63), IgG hinge, CD28 transmembrane domain, a 4-1BB costimulatory domain, and a CD3ζ chain, was previously developed and evaluated in the lab. The second-generation GD2.BBz CAR, consisting of a GD2-specific scFv (14g2a), CD8a spacer and transmembrane domain, a 4-1BB intracellular signaling domain, and a CD3ζ chain, is a gift from the laboratory of Dr. Cliona M Rooney.

Cells and culture conditions

CHLA255 cell line expressing GFP and firefly luciferase (GHLA255-GFP.FFluc) is a gift from Dr. Leonid Metelitsa and was engineered using CRISPR/Cas9 to knock out the β2m gene. K562 cell line expressing costimulatory ligands (K562-CS) and lymphoblastoid cell lines (LCLs) were a gift from the laboratory of Dr. Cliona M Rooney. NALM6 cell line expressing GFP and firefly luciferase (a gift from Dr. S Gottschalk) was engineered using CRISPR/Cas9 to knock out the β2m gene. K562 expressing OKT3 scFv (K562.OKT3) was previously generated in the laboratory. Other cell lines were obtained from ATCC. All cell lines were maintained in culture conditions recommended by ATCC. All cell lines have been routinely tested for mycoplasma.

Peripheral blood mononuclear cells (PBMC) were isolated from healthy donors' peripheral blood using Lymphoprep (Axis-Shield PoC AS) after informed consent on protocol (H-15152) approved by the Institutional Review Board at the Baylor College of Medicine, and conducted in accordance with the Declaration of Helsinki, the Belmont Report, and U.S. Common Rule. Both male and female donors (age range 20-40) were recruited.

To obtain activated T cells, isolated PBMC were plated in 24-well non-tissue culture-treated plates coated with OKT3 (1 mg/mL; Ortho Biotech) and NA/LE anti-human CD28 antibodies (1 mg/mL; BD Pharmingen) at a density of 1×10^6 cells per well. Primary human T cells were cultured in complete CTL medium containing 45% RPMI-1640 media (Hyclone Laboratories), 45% Click's medium (Irvine Scientific), 10% heat-inactivated FBS (Hyclone Laboratories), 100U/mL Pen Strep (Gibco by Life Technologies), and 2 mmol/ glutaMAX (Gibco by Life Technologies) supplemented with recombinant human IL-7 (10 ng/mL) and IL-15 (10 ng/mL).

Multivirus-specific T cells (VST)

To generate VST, human PBMC were plated in complete CTL medium with the following viral peptide mixtures (pepmix) at 1 ng/μL (10 ng per pepmix per 10^6 PBMC): Hexon, Penton, pp65, IE-1, EBNA-1, LMP1, and LMP2. The cells were cultured for 9 days before secondary stimulation. For secondary stimulation, cells were mixed with irradiated autologous activated T cells pulsed with viral pepmix (30 Gy) and irradiated K562-CS (100 Gy) at a cellular ratio of 1:1:3. On day 7 after secondary stimulation, cells were used for downstream experiments.

For tri-cultures of VST, LCLs and ADR T cells, VST were labeled with Cell Proliferation Dye eFluor™ 450 (1 μM; Invitrogen). LCLs were first incubated with the above 7-peptide mixture (10 ng per pepmix per 10^6 LCLs) for 1 hour in the incubator and then labeled with Cell Proliferation Dye eFluor™ 670 (1 μM; Invitrogen). At each time point, cells were harvested, and the remaining cell counts were quantified by flow cytometry using CountBright™ Absolute Counting Beads (Invitrogen).

Generation of gammaretroviral vectors and T-cell transduction

Retroviral supernatant was made from 293T cells as previously described[44]. Gammaretroviral supernatant was added to 24-well non-tissue culture-treated plates

precoated with retronectin (Takara Bio Inc.). Co-transduction of CAR and ADR were performed by mixing respective viral supernatants at a 1:1 volume in retronectin-coated wells. The plates were spun down at $4{,}000 \times g$ for an hour. OKT3/αCD28-activated T cells $(0.1{\text -}0.2 \times 10^6/mL$; day 2-3 after activation) resuspended in 2 mL of complete CTL medium were added to each well and centrifuged at $1000 \times g$ for 10 minutes. Transduced cells were transferred to and maintained in tissue culture-treated plates or flasks with regular media change and passaging every 2-3 days.

T-cell expansion assay

T cells were transduced on day 3 post initial activation at 0.2×10^6 per well and manually counted on day 7 and 14 using Trypan blue.

Flow cytometry

The following antibodies (clone name, catalog number) and dyes were used in this study. From BD Biosciences: APC-CD107a (clone H4A3, cat# 560664); FITC-HLAA2 (clone BB7.2, cat# 551285); FITC-HLAABC (clone G46-2.6, cat# 555552); PE-HLAABC (clone G46-2.6, cat# 555553); PerCP-CD8 (clone SK1, cat# 347314); PE-Cy7-CD19 (clone SJ25C1, cat# 557835); PE-4-1BB (clone 4B4-1, cat# 555956); FITC-TCRα/β (clone WT31, cat# 340883); PE-Cy7-CD4 (clone L200, cat# 560644); PerCP-CD4 (clone SK3, cat# 347324); PE-CD3 (clone SK7, cat# 347347); V450-granzyme B (clone GB11, cat# 561151); PE-Annexin V (cat# 556421); 7-AAD (cat# 559925); Fixable Viability Stain 700 (cat# 564997). From BioLegend: Pacific Blue-HLAA2 (clone BB7.2, cat# 343312); APC-4-1BB (clone 4B4-1, cat# 309809); LEAF™ Purified anti-human CD178 (clone NOK-1, cat# 306409); PE-Cy7-NGFR (clone ME20.4, cat# 345110). From Beckman Coulter: PC5.5-CD56 (clone N901, cat# A79388); PC5.5-CD3 (clone UCHT1, cat# A66327); APC-CD3 (clone UCHT1, cat# IM2467U); APC-A750-CD3 (clone UCHT1, cat# A66329); APC-CD45 (clone J33, cat# IM2473U); APC-CD19 (clone J3-119, cat# IM2470U); PB-CD4 (clone 13B8.2, cat# A82789); PB-CD8 (clone B9.11, cat# A82791); KrO-CD4 (clone 13B8.2, cat# A96417); KrO-CD8 (clone B9.11, cat# B00067). From Invitrogen: Cell Proliferation Dye eFluor™ 670 (cat# 65-0840-90); Cell Proliferation Dye eFluor™ 450 (cat# 65-0842-85); CellTrace™ CFSE dye (cat# C34554).

For detection of ADR on cell surface, an Alexa Fluor 647 AffiniPure Goat Anti-Human IgG, Fcγ fragment specific antibody was used (Jackson ImmunoResearch, cat# 109-605-098). Samples were acquired on either Canto II (BD Biosciences) or Gallios (Beckman Coulter) flow cytometer and analyzed using FlowJo 10 software (FlowJo LLC).

Cytotoxicity assays

T cells were cocultured with target cells at the specified E:T ratios in 200 μL complete CTL medium in the absence of cytokines, in flat-bottom 96-well plates. To generate activated T-cell targets, PBMC were activated by plate-bound OKT3 (1 mg/mL) and αCD28 (1 mg/mL) antibodies for 48 hours and then used for coculture. To assess the effect of ADR T cells on resting T cells, resting PBMC were used for coculture and target counts were adjusted according to the frequency of CD3$^+$ cells for each donor. For NK-cell cocultures, resting NK cells were isolated from fresh PBMC using CD56 MicroBeads enrichment and MS columns

(Miltenyi Biotech). In coculture experiments with activated NK cells, effector T cells, freshly isolated resting NK cells, and K562 cell line were mixed at a 1:1:1 cellular ratio. In some experiments, target cells were labeled with Cell Proliferation Dye eFluor™ 670 (1-2 μM; Invitrogen). At each time point, cells were harvested and further stained for cell surface markers to distinguish effector and target populations using flow cytometry. The remaining target cell counts were quantified by flow cytometry using CountBright™ Absolute Counting Beads (Invitrogen).

Degranulation assay

Allogeneic T cells (targets) were activated by plate-bound OKT3 (1 mg/mL) and αCD28 (1 mg/mL) antibodies for 48 hours and then cocultured with effector T cells at a 1:1 effector-to-target ratio (0.2×10^6 cells each) in 200 μL media in the presence of monensin (BD GolgiStop, BD Biosciences) and CD107a-APC antibody for 4 hours. Prior to coculture setup, apoptotic cells were removed using the dead-cell removal kit (Miltenyi Biotech) following manufacturer's instruction. After incubation, cells were first stained with Fixable Viability Stain 700 and other T-cell surface markers, then fixed and permeabilized using the Cytofix/Cytoperm Fixation/Permeabilization Solution Kit according to manufacturer's instruction (BD Biosciences) and stained for intracellular granzyme B expression before analyzed using a flow cytometer.

Blocking assays

Under normal killing conditions, target allogeneic T cells were activated by plate-bound OKT3 (1 mg/mL) and αCD28 (1 mg/mL) antibodies for 48 hours and cocultured with effector T cells at E:T = 5:1 in 200 μL CTL medium for 4 hours. Blockade of specific pathways were achieved by adding chemicals and blocking antibody as previously described[44]. Prior to coculture setup, apoptotic cells were removed using the dead-cell removal kit (Miltenyi Biotech) following manufacturer's instruction. After incubation, cells were stained with T-cell surface markers, as well as 7-AAD and Annexin V as per manufacturer's instruction and analyzed by flow cytometry.

Tissue microarray staining and evaluation

Tissue microarray slides were purchased from USBiolab (FDA999-1) and Cooperative Human Tissue Network (CHTN_NORM2) and stained with H&E and by immunohistochemistry (IHC) by Baylor College of Medicine Pathology & Histology Core according to their standard operating procedures. The primary 4-1BB antibody for IHC (ThermoFisher, clone BBK-2, cat# MS-621-P0) was used at a 1:100 dilution. The slides were then evaluated blind by a board-certified anatomic pathologist for immunoreactivity to 4-1BB and compared with the corresponding tissue slices stained by H&E. Images of the H&E and 4-1BB stained slides were taken at a magnification of 100X.

Gene knockout in T cells and cell lines

A single-guide RNA (sgRNA) specific for CD3ε (target sequence: CACTCACTGGAGAGTTCT) was designed using CRISPRscan and COSMID algorithms. The sgRNA for β2m is a gift from the laboratory of Dr. Cliona M Rooney. SgRNAs were

generated and gene knockout was performed as previously described[45]. For single-gene knockout, we delivered the sgRNA (0.6 μg for CD3ε; 1μg for β2m) together with 1 μg of Cas9 protein (Invitrogen) into $0.2\text{-}0.25 \times 10^6$ cells by using the Neon Transfection System (Thermo Fisher Scientific) in 10 μL of buffer R. For double-gene knockout, we delivered equal amount (0.375ug each) of CD3ε and β2m sgRNAs, together with 1 μg of Cas9 protein into $0.25\text{x}10^6$ T cells in 10 μL of buffer R. For electroporation of T cells and CHLA255-GFP.FFluc, three 1600-V 10-ms pulses were used. For NALM6-GFP.FFluc electroporation, we used three 1410-V 10-ms pulses or one 1350-V 30-ms pulse. Both protocols resulted in > 70% target-gene knockout. Following electroporation, cells were cultured in antibiotic-free media supplemented with 20% FBS for 2-3 days. Cells were then expanded in normal media.

For some applications, cells were sorted using either fluorescent or magnetic based methods. Following β2m gene knockout, CHLA255-GFP.FFluc and NALM6-GFP.FFluc cell lines were stained with PE-HLAABC antibody at 2 μl antibody per 10^6 cells and the GFP^{hi} PE$^-$ population were sort-purified using a SONY Cell Sorter SH800S. TCR^{KO} T cells were labeled by human CD3 MicroBeads and then passed through LD columns as per manufacturer's instruction (Miltenyi Biotech). β2m and TCR double-knockout T cells were first co-stained by PE-HLAABC and PE-CD3 antibodies followed by anti-PE MicroBeads, and then passed through LD columns according to manufacturer's instruction (Miltenyi Biotech). Sorting efficiency routinely exceeded 99%.

Mixed lymphocyte reaction (MLR)

Donor T cells were cocultured with freshly isolated recipient PBMC or NK cells at the specified E:T ratios in 200 μL RPMI media supplemented with 10% FBS in flat bottom 96-well plates. NK cells were removed from PBMC using human CD56 MicroBeads and LD columns as per manufacturer's instruction (Miltenyi Biotech). Purity routinely exceeded 99%. To isolate NK cells from PBMC, the EasySep™ Human NK Cell Isolation Kit (Stemcell Technologies) was used following manufacturer's instructions. In some experiments, NK cells were obtained by positive enrichment with human CD56 MicroBeads (Miltenyi Biotech). Purity of isolated NK cells was 95-99%. To generate primed alloreactive T cells, PBMC from recipients were irradiated at 30 Gy and mixed with fresh donor PBMC at 1:1 in CTL medium supplemented with 20 U/mL recombinant human IL-2. Media was changed to pure CTL medium without cytokine after 4 days. One week later, T cells were isolated using human CD3 MicroBeads and MS columns as per manufacturer's instruction (Miltenyi Biotech). Purity routinely exceeded 99%.

For MLR assays with PBMC, cells were supplemented on day 0 with 20 U/mL recombinant human IL-2. On day 4, media were changed to fresh RPMI + 10% FBS without cytokine. Media was then changed every 2-3 days (without cytokine). At each time point, cells from one well were collected and stained with anti-human CD3, HLA-ABC, HLA-A2, CD56, CD4, and CD8 antibodies to distinguish effector and target populations for flow cytometry. Cell counts were quantified by flow cytometry using CountBright™ Absolute Counting Beads (Invitrogen).

Mouse strains and study approval

Breeder pairs of *NOD.Cg-Prkdc^{scid} Il2rg^{tm1Wjl}/SzJ* mice (NSG, Stock No. 005557) and NOD.Cg-*Prkdc^{scid} H2-Ab1^{em1Mvw} H2-K1^{tm1Bpe} H2-D1^{tm1Bpe} Il2rg^{tm1Wjl}*/SzJ mice (NSG (MHC^{null}), Stock No. 025216) were purchased from The Jackson Laboratory and bred in Baylor College of Medicine animal facility. Both female and male littermates (8 to 12-week-old) were used for experiments. All animal experiments were conducted in compliance with the Baylor College of Medicine IACUC (Protocol #AN-4758).

In vivo T cell-mediated rejection model

NSG mice were irradiated at 1.2 Gy on day −1, and on the following day received 7×10^6 *in vitro* expanded human T cells (day 8-10 post initial OKT3/αCD28 stimulation) from an HLA-A2$^+$ recipient. Four days later, mice received 2×10^6 non-transduced or ADR-expressing T cells from an HLA-A2$^-$ donor intravenously. To track expansion of donor and recipient T cells *in vivo*, 50 μL of peripheral blood was obtained by tail-vein bleeding at specified time points. After red blood cell lysis, samples were stained with anti-human CD45, CD3, and HLA-A2 antibodies for flow cytometry analysis.

For re-challenge experiments, *in vitro* expanded human T cells from both A2$^+$ and A2$^-$ donors were mixed at a 1:1 ratio, labeled with CFSE dye (Invitrogen) and intravenously injected into mice at 4×10^6 total cells per mouse. Forty-eight hours later, mice were euthanized, blood and spleen were collected post-mortem. Blood and splenocytes were then treated with ACK lysis buffer and stained with anti-human CD45, CD3, and HLA-A2 antibodies for flow cytometry analysis.

To evaluate residual alloreactivity of recipient T cells following ADR T-cell administration, HLA-A2$^+$ recipient T cells were isolated >80 days after injection from spleens of mice using Lymphoprep (Axis-Shield PoC AS) followed by magnetic based enrichment (Miltenyi Biotech). Purified cells were >95% HLA-A2$^+$ and were cocultured with a 1:1 mix of eFluor670 dye (Invitrogen) labeled TCR^{KO} T cells from both donor and recipient. As a control, purified T cells were cocultured with K562.OKT3 cells for 72 hours at E:T=2:1 for 72 hours and residual target cell counts were quantified by flow cytometry using CountBright™ Absolute Counting Beads (Invitrogen).

In vivo PBMC-mediated rejection model

NSG (MHC^{KO}) mice were irradiated at 1.2 Gy on day −1, and then received intravenously 5×10^6 freshly isolated PBMC from an HLA-A2$^+$ recipient on day 0; Four days later, 5×10^6 non-transduced or ADR-expressing T cells from an HLA-A2$^-$ donor were administered intravenously. To track expansion of both infused populations *in vivo*, 50 μL of peripheral blood was obtained by tail-vein bleeding at specified time points. After red blood cell lysis, samples were stained with anti-human CD45, CD3, and HLA-A2 antibodies for flow cytometry analysis.

Xenograft neuroblastoma model

NSG mice were irradiated at 1.2 Gy and received intravenously 7×10^6 *in vitro* expanded human T cells (day 8-10 post initial OKT3/αCD28 stimulation) from an HLA-A2$^+$ recipient

on the following day. Twenty-four hours later, 1×10^6 CHLA255-GFP.FFluc ($\beta 2m^{KO}$) were injected intravenously, followed by 1×10^6 non-transduced or ADR/CAR-expressing T cells generated from an HLA-A2$^-$ donor three days later. T-cell expansion was monitored by blood analysis as described above. Tumor progression was measured by injecting mice intraperitoneally with 100 μL D-luciferin (30 mg/mL, PerkinElmer Inc.) followed by bioluminescence imaging using an IVIS Lumina II imaging system and analyzed by Living Image 4.5 software (Caliper Life Sciences). Mice were euthanized when developed signs of excessive tumor burden or when weight loss exceeded 20% of baseline.

Xenograft B-cell leukemia model

NSG mice were irradiated at 0.8 Gy or 1.2 Gy, where indicated, and received intravenously 7×10^6 *in vitro* expanded human T cells (day 8-10 post initial OKT3/αCD28 stimulation) from an HLA-A2$^+$ recipient on the following day; Twenty-four hours later, 1×10^6 NALM6-GFP.FFluc ($\beta 2m^{KO}$) were injected intravenously, followed by 2×10^6 (wildtype) or 3×10^6 (TCR^{KO}) non-transduced or ADR/CAR-expressing T cells generated from an HLA-A2$^-$ donor three days later. T-cell expansion and tumor progression was monitored as described above. Mice were euthanized when developed signs of excessive tumor burden or when weight loss exceeded 20% of baseline.

In vivo ADR T-cell persistence model

NSG mice were irradiated at 1.2 Gy on day -1 and received 7×10^6 *in vitro* expanded human T cells (day 8-10 post initial OKT3/αCD28 stimulation) from an HLA-A2$^+$ recipient on the following day. Four days later, mice received 2×10^6 ADR-expressing T cells from an HLA-A2$^-$ donor intravenously. To track expansion of both infused populations *in vivo*, 50 μL of peripheral blood was obtained by tail-vein bleeding at specified time points. After red blood cell lysis, samples were stained with anti-human CD45, CD3, and HLA-A2 antibodies for flow cytometry analysis.

In vivo CAR.ADR T-cell persistence model

NSG (MHC^{KO}) mice were irradiated at 1.2 Gy on day -1, and then received intravenously 3×10^6 FFluc labeled TCR^{KO} CD19 CAR T cells or CD19 CAR.ADR T cells on day 5. At specified time points, T-cell expansion was measured by injecting mice intraperitoneally with 100 μL D-luciferin (30 mg/mL, PerkinElmer Inc.) followed by bioluminescence imaging using an IVIS Lumina II imaging system and analyzed by Living Image 4.5 software (Caliper Life Sciences).

Statistics

Statistical significance involving two groups was determined by either paired *t* test (when control and experimental T cells were generated from the same set of PBMC donors) or unpaired Student's t test (when T cells in two groups were not entirely donor-matched). For comparisons in time courses or among 3 groups or more, ANOVA followed by multiple comparisons were used and adjusted *p* values were calculated using Tukey's or Sidak's correction, where indicated. Statistical significance in Kaplan-Meier survival curves was

assessed by the Mantel-Cox log-rank test. All *p* values were calculated using Prism 6 software (GraphPad). Error bars show SD in all graphs.

Data availability

All data generated for this manuscript will be made available upon reasonable request to the corresponding author.

Supplementary Material

Refer to Web version on PubMed Central for supplementary material.

Acknowledgements

References

1. June CH & Sadelain M Chimeric Antigen Receptor Therapy. N. Engl. J. Med 379, 64–73 (2018). [PubMed: 29972754]

2. Papadopoulou A et al. Activity of broad-spectrum T cells as treatment for AdV, EBV, CMV, BKV, and HHV6 infections after HSCT. Sci. Transl. Med 6, 242ra83 (2014).

3. Turtle CJ et al. Immunotherapy of non-Hodgkin's lymphoma with a defined ratio of CD8+ and CD4+ CD19-specific chimeric antigen receptor–modified T cells. Sci. Transl. Med 8, 355ra116–355ra116 (2016).

4. Graham C et al. Allogeneic CAR-T Cells: More than Ease of Access? Cells 7, 155 (2018).

5. Torikai H et al. A foundation for universal T-cell based immunotherapy: T cells engineered to express a CD19-specific chimeric-antigen-receptor and eliminate expression of endogenous TCR. Blood 119, 5697–5705 (2012). [PubMed: 22535661]

6. Qasim W et al. Molecular remission of infant B-ALL after infusion of universal TALEN gene-edited CAR T cells. Sci. Transl. Med 9, eaaj2013 (2017). [PubMed: 28123068]

7. Ren J et al. Multiplex Genome Editing to Generate Universal CAR T Cells Resistant to PD1 Inhibition. Clin. Cancer Res 23, 2255–2266 (2017). [PubMed: 27815355]

8. Eyquem J et al. Targeting a CAR to the TRAC locus with CRISPR/Cas9 enhances tumour rejection. Nature 543, 113–117 (2017). [PubMed: 28225754]

9. Poirot L et al. Multiplex Genome-Edited T-cell Manufacturing Platform for 'Off-the-Shelf' Adoptive T-cell Immunotherapies. Cancer Res. 75, 3853–3864 (2015). [PubMed: 26183927]

10. Tzannou I et al. Off-the-Shelf Virus-Specific T Cells to Treat BK Virus, Human Herpesvirus 6, Cytomegalovirus, Epstein-Barr Virus, and Adenovirus Infections After Allogeneic Hematopoietic Stem-Cell Transplantation. J. Clin. Oncol 35, 3547–3557 (2017). [PubMed: 28783452]

11. Leen AM et al. Multicenter study of banked third-party virus-specific T cells to treat severe viral infections after hematopoietic stem cell transplantation. Blood 121, 5113–5123 (2013). [PubMed: 23610374]

12. Melenhorst JJ et al. Allogeneic virus-specific T cells with HLA alloreactivity do not produce GVHD in human subjects. Blood 116, 4700–4702 (2010). [PubMed: 20709906]

13. Watts TH TNF/TNFR FAMILY MEMBERS IN COSTIMULATION OF T CELL RESPONSES. Annu. Rev. Immunol 23, 23–68 (2005). [PubMed: 15771565]

14. Elliott TJ & Eisen HN Allorecognition of purified major histocompatibility complex glycoproteins by cytotoxic T lymphocytes. Proc. Natl. Acad. Sci 85, 2728–2732 (1988). [PubMed: 2451830]

15. Ciccone E et al. Evidence of a natural killer (NK) cell repertoire for (allo) antigen recognition: definition of five distinct NK-determined allospecificities in humans. J. Exp. Med 175, 709–18 (1992). [PubMed: 1371301]

16. Ruggeri L et al. Effectiveness of Donor Natural Killer Cell Alloreactivity in Mismatched Hematopoietic Transplants. Science (80-.). 295, 2097–2100 (2002).

17. Colonna M, Brooks E, Falco M, Ferrara G & Strominger J Generation of allospecific natural killer cells by stimulation across a polymorphism of HLA-C. Science (80-.). 260, 1121–1124 (1993).

18. Torikai H et al. Toward eliminating HLA class I expression to generate universal cells from allogeneic donors. Blood 122, 1341–1349 (2013). [PubMed: 23741009]

19. Storkus WJ, Howell DN, Salter RD, Dawson JR & Cresswell P NK susceptibility varies inversely with target cell class I HLA antigen expression. J. Immunol 138, 1657–9 (1987). [PubMed: 3819393]

20. Brehm MA et al. Lack of acute xenogeneic graft-versus-host disease, but retention of T-cell function following engraftment of human peripheral blood mononuclear cells in NSG mice deficient in MHC class I and II expression. FASEB J. 33, 3137–3151 (2019). [PubMed: 30383447]

21. Tian G et al. CD62L+ NKT cells have prolonged persistence and antitumor activity in vivo. J. Clin. Invest 126, 2341–55 (2016). [PubMed: 27183388]

22. Lamers CHJ et al. Immune responses to transgene and retroviral vector in patients treated with ex vivo-engineered T cells. Blood 117, 72–82 (2011). [PubMed: 20889925]

23. Maus MV et al. T cells expressing chimeric antigen receptors can cause anaphylaxis in humans. Cancer Immunol. Res 1, 26–31 (2013).

24. Sommermeyer D et al. Fully human CD19-specific chimeric antigen receptors for T-cell therapy. Leukemia 31, 2191–2199 (2017). [PubMed: 28202953]

25. Gornalusse GG et al. HLA-E-expressing pluripotent stem cells escape allogeneic responses and lysis by NK cells. Nat. Biotechnol 35, 765–772 (2017). [PubMed: 28504668]

26. Braud VM et al. HLA-E binds to natural killer cell receptors CD94/NKG2A, B and C. Nature 391, 795–799 (1998). [PubMed: 9486650]

27. Lee N et al. HLA-E is a major ligand for the natural killer inhibitory receptor CD94/NKG2A. Proc. Natl. Acad. Sci 95, 5199–5204 (1998). [PubMed: 9560253]

28. Lieto LD, Maasho K, West D, Borrego F & Coligan JE The human CD94 gene encodes multiple, expressible transcripts including a new partner of NKG2A/B. Genes Immun. 7, 36–43 (2006). [PubMed: 16237464]

29. Schwarz H, Valbracht J, Tuckwell J, von Kempis J & Lotz M ILA, the human 4-1BB homologue, is inducible in lymphoid and other cell lineages. Blood 85, 1043–52 (1995). [PubMed: 7849293]

30. Zhang X et al. CD137 promotes proliferation and survival of human B cells. J. Immunol 184, 787–95 (2010). [PubMed: 20008291]

31. Pauly S, Broll K, Wittmann M, Giegerich G & Schwarz H CD137 is expressed by follicular dendritic cells and costimulates B lymphocyte activation in germinal centers. J. Leukoc. Biol 72, 35–42 (2002). [PubMed: 12101260]

32. Alfaro C et al. Functional expression of CD137 (4-1BB) on T helper follicular cells. Oncoimmunology 4, e1054597 (2015). [PubMed: 26587331]

33. Heinisch IVWM, Bizer C, Volgger W & Simon H-U Functional CD137 receptors are expressed by eosinophils from patients with IgE-mediated allergic responses but not by eosinophils from patients with non–IgE-mediated eosinophilic disorders☆. J. Allergy Clin. Immunol 108, 21–28 (2001). [PubMed: 11447378]

34. Nakajima T et al. Marked increase in CC chemokine gene expression in both human and mouse mast cell transcriptomes following Fcepsilon receptor I cross-linking: an interspecies comparison. Blood 100, 3861–3868 (2002). [PubMed: 12393595]

35. Sallusto F, Lenig D, Förster R, Lipp M & Lanzavecchia A Two subsets of memory T lymphocytes with distinct homing potentials and effector functions. Nature 401, 708–712 (1999). [PubMed: 10537110]

36. Cheuk S et al. CD49a Expression Defines Tissue-Resident CD8+ T Cells Poised for Cytotoxic Function in Human Skin. Immunity 46, 287–300 (2017). [PubMed: 28214226]

37. Casey KA et al. Antigen-independent differentiation and maintenance of effector-like resident memory T cells in tissues. J. Immunol 188, 4866–75 (2012). [PubMed: 22504644]

38. Ramos CA et al. Clinical and immunological responses after CD30-specific chimeric antigen receptor-redirected lymphocytes. J. Clin. Invest 127, 3462–3471 (2017). [PubMed: 28805662]

39. Ruella M et al. Induction of resistance to chimeric antigen receptor T cell therapy by transduction of a single leukemic B cell. Nat. Med 24, 1499–1503 (2018). [PubMed: 30275568]

40. Zhao Z et al. Structural Design of Engineered Costimulation Determines Tumor Rejection Kinetics and Persistence of CAR T Cells. Cancer Cell 28, 415–428 (2015). [PubMed: 26461090]

41. Menk AV et al. 4-1BB costimulation induces T cell mitochondrial function and biogenesis enabling cancer immunotherapeutic responses. J. Exp. Med 215, 1091–1100 (2018). [PubMed: 29511066]

42. Stephan MT et al. T cell–encoded CD80 and 4-1BBL induce auto- and transcostimulation, resulting in potent tumor rejection. Nat. Med 13, 1440–1449 (2007). [PubMed: 18026115]

Methods-only references

43. Mamonkin M et al. Reversible Transgene Expression Reduces Fratricide and Permits 4-1BB Costimulation of CAR T Cells Directed to T-cell Malignancies. Cancer Immunol. Res 6, 47–58 (2018). [PubMed: 29079655]

44. Mamonkin M, Rouce RH, Tashiro H & Brenner MK A T-cell-directed chimeric antigen receptor for the selective treatment of T-cell malignancies. Blood 126, 983–992 (2015). [PubMed: 26056165]

45. Gomes-Silva D et al. CD7-edited T cells expressing a CD7-specific CAR for the therapy of T-cell malignancies. Blood 130, 285–296 (2017). [PubMed: 28539325]

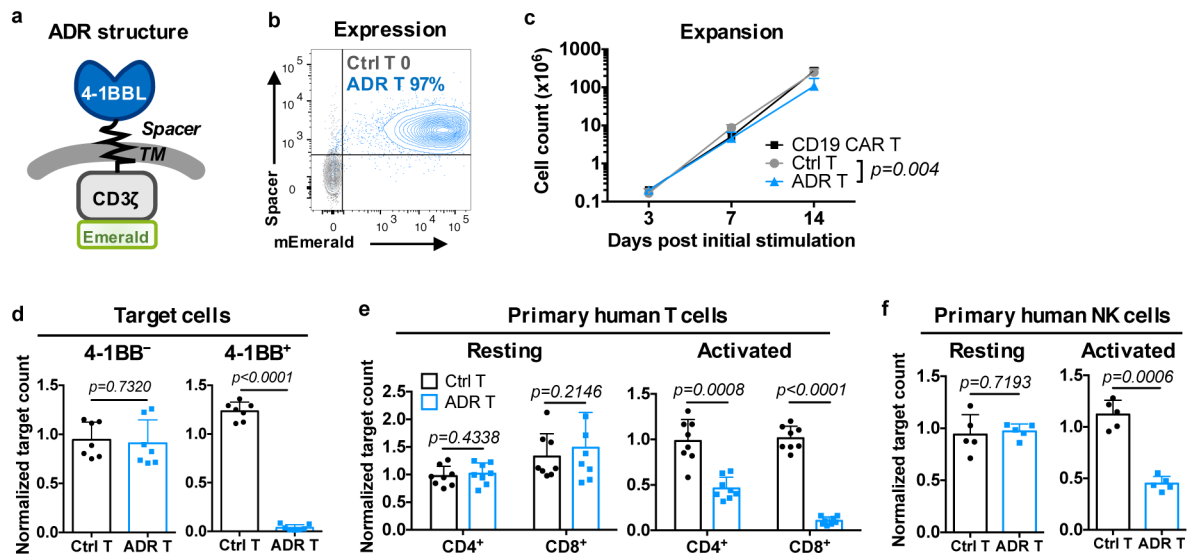**Figure 1. 4-1BB-specific ADR T cells selectively eliminate activated T and NK cells *in vitro*.**
a, Schematic of the ADR structure. TM, transmembrane domain. **b,** ADR expression on the surface of primary human T cells (ADR T, blue). Non-transduced T cells were used as control (Ctrl, grey). Data are representative of >50 independent experiments with 12 different donors. **c,** Counts of activated human T cells following mock transduction (Ctrl T) or gammaretroviral transduction with CD19 CAR or ADR (n=6). *P* value for the comparison of Ctrl T and ADR T group on day 14 was shown and was calculated by one-way ANOVA with Holm correction for multiple comparisons. **d-f,** Non-transduced (Ctrl) or ADR T cells were cocultured with 4-1BB$^-$ cell line NALM6 (**d**, left), 4-1BB$^+$ cell line HDLM2 (**d**, right), autologous resting T cells (**e**, left), pre-activated T cells (**e**, right), resting NK cells (**f**, left), or pre-activated NK cells (**f**, right) at a 1:1 effector-to-target ratio for 24 hours. Residual target cells were quantified by flow cytometry and normalized to the target-only condition. In **d**-**f**, data denote mean±SD with individual data points obtained from different donors shown on each graph. *P* values were determined by two-tailed paired *t* test.
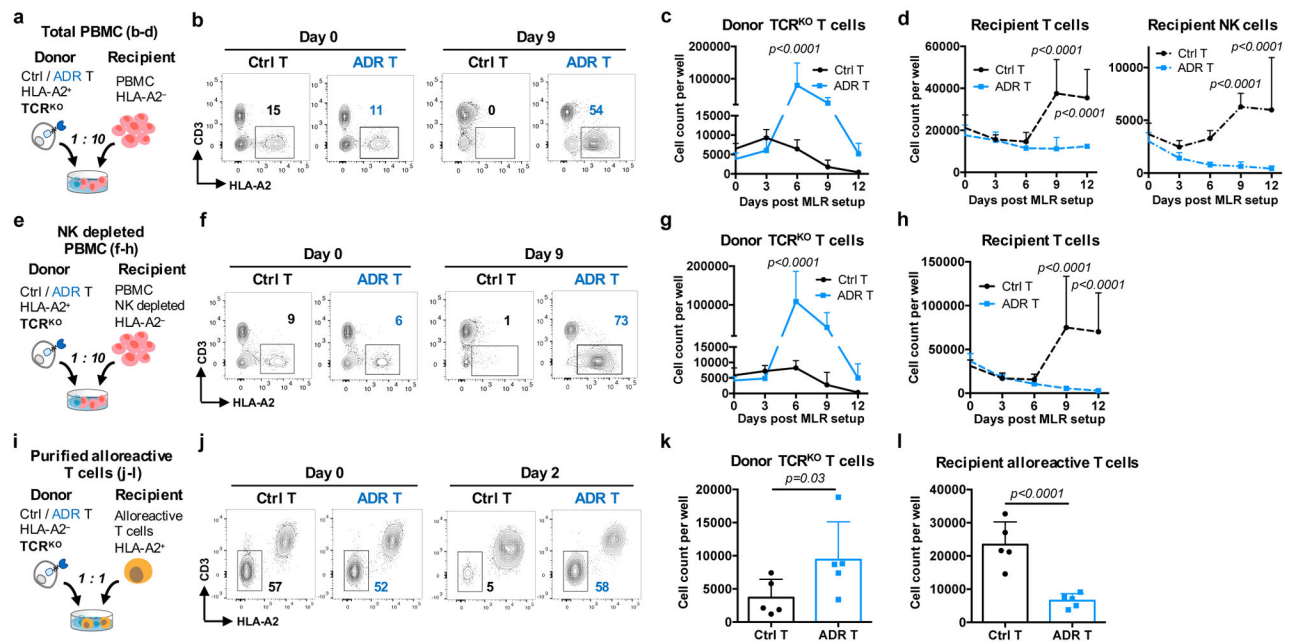
Figure 2. ADR protects T cells from T-cell mediated rejection *in vitro*.
a, Schematic of model setup for **b-d**. Non-transduced (Ctrl) or ADR-transduced donor TCR^KO HLA-A2^+ T cells were mixed with mismatched recipient's whole PBMC at a 1:10 cell ratio. **b,** Representative flow plots showing total frequency of donor T cells on day 0 and day 9 of coculture. **c-d,** Absolute counts of donor T cells (**c**), recipient T cells (**d,** left) and recipient NK cells (**d,** right) during coculture. **e,** Schematic of model setup for **f-h**. Donor TCR^KO T cells and recipient NK-depleted PBMC were mixed at a 1:10 cell ratio. Non-transduced TCR^KO T cells were used as control (Ctrl T). **f,** Representative flow plots showing percentage of CD3^− HLA-A2^+ donor T cells within total alive cells on day 0 and day 9 after coculture setup. **g-h,** Absolute cell counts of CD3^− HLA-A2^+ donor TCR^KO T cells (**g**) and recipient CD3^+ HLA-A2^− T cells (**h**) at specified days after coculture setup. **i,** Schematic of model setup for **j-l**. Donor TCR^KO T cells were mixed with primed recipient alloreactive T cells at a 1:1 ratio. **j,** Representative flow plots showing percentage of donor T cells on day 0 and day 2 of coculture. **k-l,** Absolute cell counts of donor T cells (**k**), recipient alloreactive T cells (**l**) on day 2 of coculture. All data denote mean±SD. In **a-h**, 6 unique donor-recipient pairs were used. *P* values were determined by two-way ANOVA with Sidak correction for multiple comparisons, non-significant (*p*>0.05) values are not shown. In **k-l,** each dot represents a unique donor-recipient pair, and *p* values were determined by a two-tailed paired Student's *t* test.
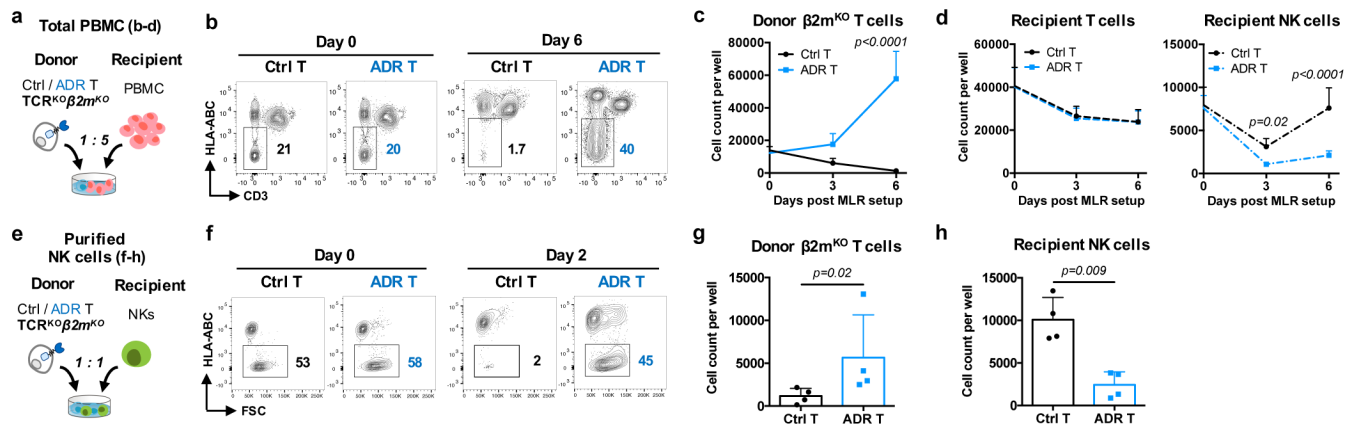
Figure 3. ADR protects T cells from NK-cell mediated rejection *in vitro*.
a, Schematic of model setup for **b-d**. Donor $TCR^{KO}\beta2m^{KO}$ T cells and recipient whole PBMC were mixed at a 1:5 ratio. **b,** Representative flow plots showing percentage of donor T cells on day 0 and day 6 of coculture setup. **c-d,** Absolute cell counts of HLA-ABC⁻ donor T cells (**c**), recipient HLA-ABC⁺ T cells (**d,** left) and recipient CD56⁺ HLA-ABC⁺ NK cells (**d,** right) during coculture. **e,** Schematic of model setup for **f-h**. Donor $TCR^{KO}\beta2m^{KO}$ T cells were mixed with freshly isolated recipient NK cells at a 1:1 ratio. **f,** Representative flow plots showing total frequency of donor T cells on day 0 and day 2 of coculture. **g-h,** Absolute cell counts of donor T cells (**g**) and recipient NK cells (**h**) on day 3 of coculture. All data denote mean±SD. In **c-d**, 5 unique donor-recipient pairs were used. *P* values were determined by two-way ANOVA with Sidak correction for multiple comparisons and non-significant (*p*>0.05) values are not shown. In **g-h**, each dot represents a unique donor-recipient pair, and *p* values were determined by two-tailed paired *t* test.
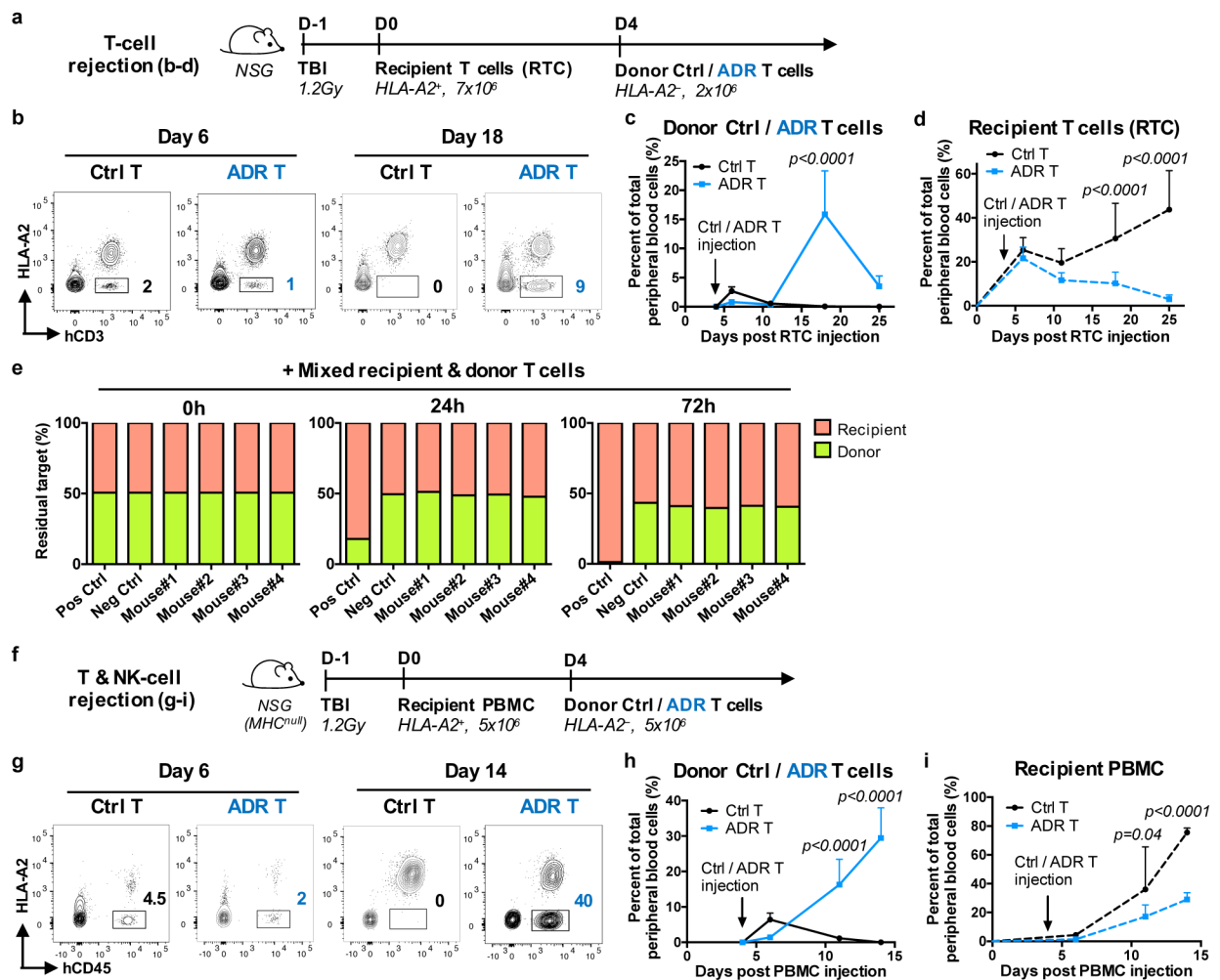
Figure 4. ADR T cells are protected from allogeneic rejection *in vivo*.
a, Schematic of model setup for **b-d** (Ctrl, n=5; ADR, n=7). RTC, recipient T cells. **b,** Representative flow plots showing frequencies of donor HLA-A2⁻ Ctrl or ADR T cells in peripheral blood of mice on days 6 and 18. **c-d,** Frequencies of donor HLA-A2⁻ T cells **(c)** and recipient HLA-A2⁺ T cells **(d)** at specified time points. **e,** Isolated recipient T cells from mice that had previously received ADR T cells were cocultured with a 1:1 mix of donor and recipient TCR^KO T cells at a 2:1 effector-to-target ratio for 72 hours. The donor:recipient cell ratio was assessed at indicated times during coculture. Recipient T cells primed *in vitro* against irradiated donor cells were used as a positive control (Pos Ctrl) and a mix of targets alone as a negative control (Neg Ctrl). **f,** Schematic of model setup for **g-I,** (Ctrl, n=4; ADR, n=5). **g,** Representative flow plots showing percentage of donor Ctrl or ADR T cells in peripheral blood on day 6 and 14. **h-i,** Frequencies of donor HLA-A2⁻ Ctrl or ADR T cells **(h)** and HLA-A2⁺ recipient PBMC **(i)** at specified time points. TBI, total body irradiation. In **c-d** and **h-i**, data are mean±SD. *P* values were determined via two-way ANOVA with Sidak correction for multiple comparisons, non-significant (*p*>0.05) values are not shown.
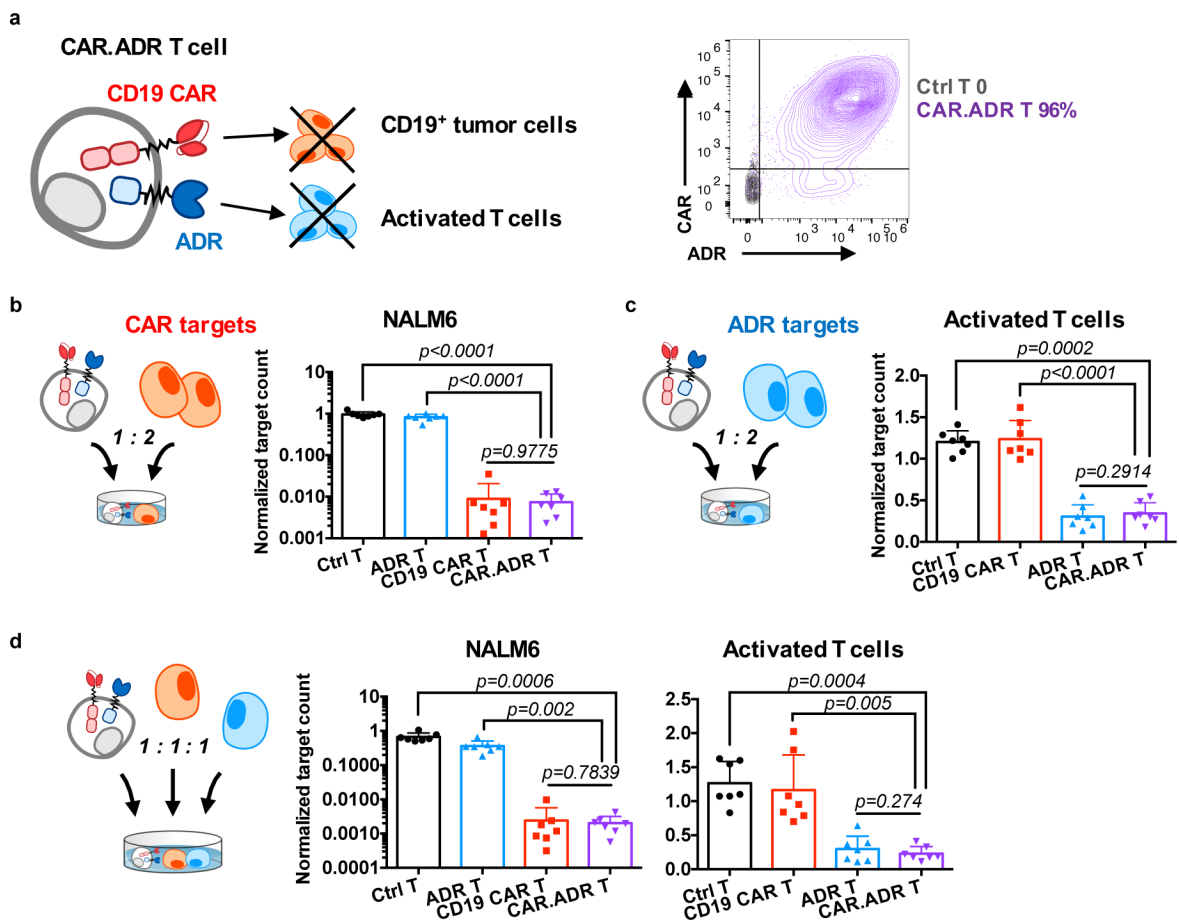
Figure 5. T cells co-expressing ADR and CAR retain function of both receptors *in vitro*.
a, Left, schematic of a CAR.ADR T cell and its respective targets. Right, representative flow plot showing co-expression of a second-generation CAR and ADR on T cell surface (purple) compared to non-transduced control (Ctrl) T cells (grey). Data are representative of >20 independent experiments with 8 individual donors. **b,** T cells expressing either CD19 CAR or ADR alone or co-expressing both receptors were cocultured with NALM6-GFP (β2m^{KO}) leukemia cells (**b**) or autologous activated T cells (**c**) at a 1:2 cell ratio for 48 hours. Residual counts of live target cells were quantified by flow cytometry at the end of coculture and normalized to target-only condition. **d,** T cells expressing either or both CAR and ADR were cocultured with a 1:1 mix of NALM6-GFP (β2m^{KO}) cells and autologous activated T cells for 48 hours. Residual normalized counts of target cells are plotted. Data from 7 individual donors are shown. All data denote mean±SD. *P* values were determined by one-way ANOVA with Tukey (**b-c**) or Holm-Sidak (**d**) correction for multiple comparisons.
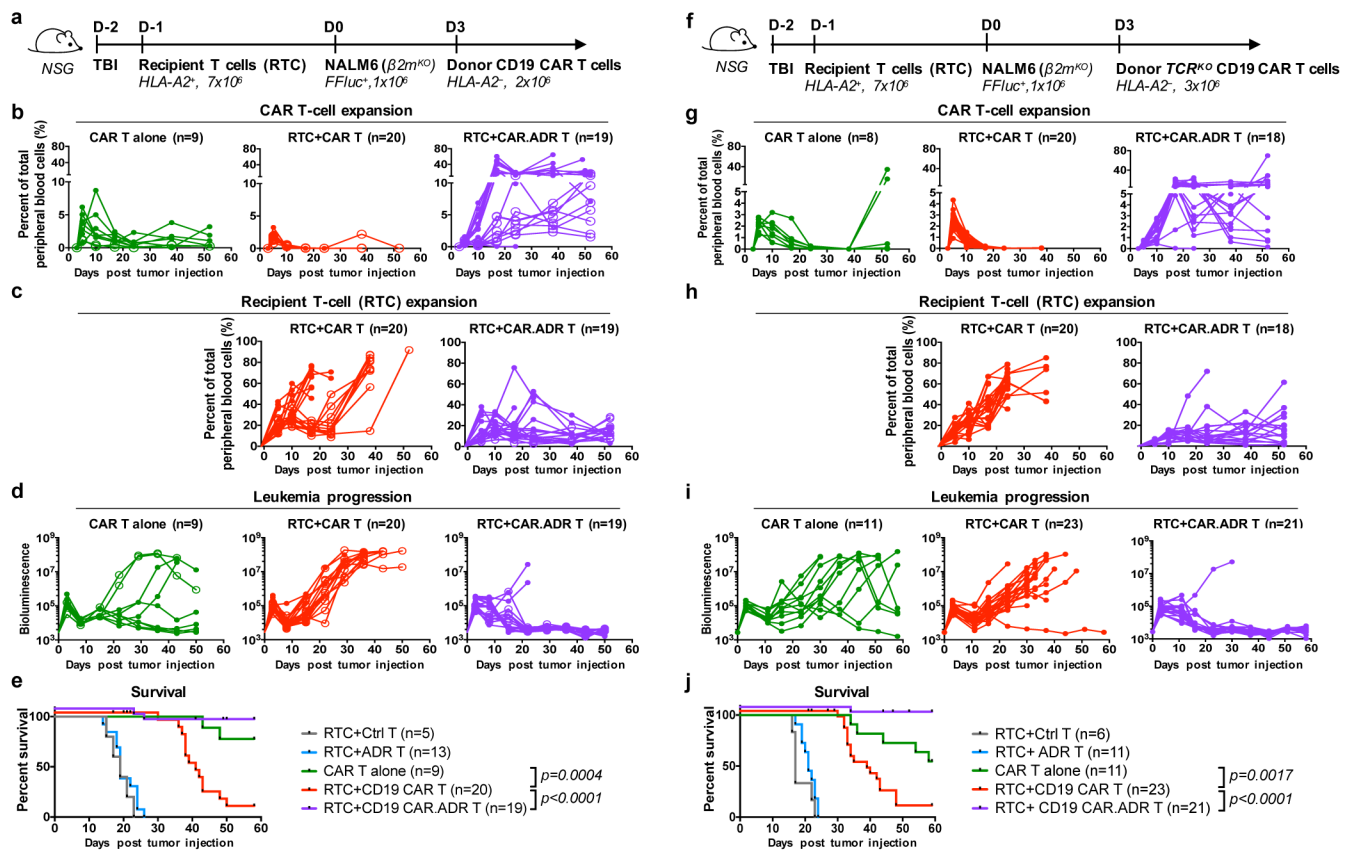
Figure 6. CD19 CAR T cells co-expressing ADR resist alloimmune rejection *in vivo* and retain potent anti-tumor function.

a, Schematic of the mouse model. All cell injections were performed intravenously. **b-c,** Frequencies of HLA-A2⁻ donor CAR T cells (**b**) and HLA-A2⁺ recipient T cells (RTC) (**c**) in peripheral blood after tumor injection. CAR T alone, CD19 CAR T cells were given to leukemia-bearing mice without pre-engrafted recipient T cells **d,** Leukemia progression measured using IVIS imaging at specified time points. Individual lines denote data obtained from each animal. Open circles denote mice receiving 0.8Gy TBI while solid circles denote mice receiving 1.2Gy TBI on day −2. **e,** Kaplan-Meier curve showing overall animal survival in each experimental group. **f,** Schematic of the mouse model for **g-j**. **g-h,** Frequencies of donor HLA-A2⁻ CAR T cells (**g**) and HLA-A2⁺ recipient T cells (RTC) (**h**) in peripheral blood cells of individual animals. **i,** Tumor bioluminescence signals measured at specified time points. **j,** Kaplan-Meier curve showing survival of mice in each experimental group. *P* values were determined by two-sided log-rank test.